

# Syngas-fed cogeneration for the tertiary sector: lessons learned from the Synbiose project

**Andrea Borghi<sup>a</sup>, Nicola Casari<sup>b</sup>, Agostino Gambarotta<sup>c</sup>, Edoardo Micconi<sup>a</sup>,  
Mirko Morini<sup>c</sup>, Michele Pinelli<sup>b</sup> and Alessio Suman<sup>b</sup>**

<sup>a</sup> *Siram Veolia, Milan, Italy, andrea.borghi@veolia.com edoardo.micconi@veolia.com*

<sup>b</sup> *University of Ferrara, Ferrara, Italy, nicola.casari@unife.it michele.pinelli@unife.it  
alessio.suman@unife.it*

<sup>c</sup> *University of Parma, Parma, Italy, agostino.gambarotta@unipr.it mirko.morini@unipr.it CA*

## Abstract:

Within the strategies for sustainable transition and decarbonization, biomass gasification represents an interesting solution to yield renewable fuels that can be used in internal combustion plants for power and combined heat and power (CHP) generation. The use of syngas instead of original biomasses allows industrial internal combustion engines to achieve higher conversion efficiencies and lower pollutant emissions. However, limited experience on real operative plants has led to a lower diffusion of the technology than expected.

To investigate the real behavior of a gasifier fed with lignocellulosic woodchips and coupled with a CHP engine, a commercial-grade system has been installed in the Science and Technologies Campus of the University of Parma. The aim of the research project Synbiose was to gain a better understanding of the processes to enhance the application of small-scale gasification and CHP plants in the tertiary sector. Operating parameters of the system – properly instrumented – have been monitored to analyze its performance and to improve its maintainability. In order to investigate the effects of woodchips from different tree species on system performance, a second smaller plant was built and has been used for a specific experimental activity.

An extended modelling study has been developed to enhance the comprehension of the gasification process and of the plant operation. A hybrid thermochemical model has been used for the simulation of the gasification process, while a lumped parameter dynamic model and multiphase CFD simulations have been applied and integrated to analyze the operation of the whole plant.

The aim of the paper is to summarize the results of these research activities highlighting the issues that arose during the project with specific reference to the implemented solutions.

## Keywords:

Biomass; Cogeneration; Experimentation; Gasification; Simulation.

## 1. Introduction

Renewable energy sources play a key role in the sustainable transition and decarbonization of the power system. Together with solar and wind technologies (which are typically non-programmable), biomasses represent an interesting way to exploit the use of renewable energy without having relevant storage issues.

Currently, biomasses are used for direct combustion in combined heat and power (CHP) steam plants (i.e. wooden biomass direct combustion, giving rise to noteworthy issues of pollutant formation), or they are converted into so-called biogas through anaerobic fermentation that can be used as fuel for CHP plants based on internal combustion engines or micro-gas turbines. In both cases the size and flexibility of the comprehensive conversion and generation plants hinder their applications in the tertiary sector (e.g. hospitals, university campuses).

Within this context, the gasification process of wooden biomasses is an interesting alternative allowing for the production of a gaseous fuel (syngas) that can be properly cleaned and used for CHP generation. Moreover, the use of thermochemical conversion and of internal combustion engines allows for smaller and more flexible plants, which can use locally available solid biomasses more efficiently.

However, the lack of field testing knowledge on these plants (with particular reference to operation and maintenance issues and to syngas production and cleaning technologies) still seems to limit their use in real applications. In the current Italian context, almost no small-size syngas-fed operating CHP plants can be found on which adequate operating experience has been acquired to evaluate their performance and reliability.

To overcome this issue, the Synbio project has been started with the aim of enhancing the theoretical and experimental comprehension of small-scale gasification-CHP plants to allow for their wider application in the tertiary sector. The project lasted from February 2017 to May 2021 and involved the installation, instrumentation, testing and modelling of a commercial-grade plant based on a gasifier fed with lignocellulosic woodchips. The project partners were Siram S.p.A., the Center for Energy and Environment-CIDEA of the University of Parma, and the Department of Engineering of the University of Ferrara. The plant is installed in the Campus of the University of Parma and is directly connected to the local electrical grid and to the district heating network (fed by natural gas boilers) which fulfil the demands of the Campus buildings (with a total peak heating power demand of 16 MW).

Many examples can be found in the literature regarding the optimization of the gasification process [1] and its modelling [2, 3] or regarding experimental tests [4]. There are very few examples related to applications in an operating environment [5, 6] and none with an experimental and numerical approach.

### **1.1. Aim of the paper**

The aim of this paper is to give a concise presentation of the outcomes of the activities of the 51-month project and to present a summary of the main lessons that have been learned from the experience gained. The main goal of the project was to bring the gasification technology to a sufficient level of maturity to be able to represent a viable technical solution for its application in the tertiary sector. To achieve this goal, the partners were involved in experimental and computational research which are summarized in the following sections. In particular, Section 2 presents the two plants that have been installed at the Campus and their measurement and acquisition systems.

The first plant is characterized by an installed nominal electrical power of 125 kW and it was used for long run testing to evaluate the reliability of the technology. The second, with an installed electrical nominal power of 25 kW, was instead used to evaluate the fuel flexibility of the technology by testing its operation with different tree species. The results of these experimental activities are summarized in Section 3.

Beside the experimental activity, the project also dealt with the development of the mathematical models of the process, of the whole plant and of its components. Section 4 briefly shows the mathematical model of the gasification process and its validation, the dynamic model of the whole syngas cleaning line and the CFD analyses that have been performed on relevant components.

Finally, some conclusions have been made in Section 5, wrapping up the whole project, and providing useful hints for those who will try to replicate the experience.

## **2. The plants**

The experimental equipment used in the project consists of two biomass-fueled syngas cogeneration plants (Figure 1). The sizes of these two plants, in terms of electrical power output, are 125 kW and 25 kW, respectively. Both plants are located at a dedicated facility in the Science and Technologies Campus of the University of Parma.

### **2.1. The 125-kW plant**

The plant consists of biomass storage, i.e. wood chips, which is fed by means of an auger system into a storage chamber that can guarantee an operating autonomy of the plant of approximately 3 to 4 days at maximum power. Downstream of this biomass storage site is a vibrating screener, consisting of opposing grates that allow the wood chips to be sieved in order to remove the finest fractions. These fine fractions would cause occlusions inside the gasification reactor, affecting the empty/full ratio and limiting the passage of the syngas, which would therefore not be able to flow properly inside the reactor.

The feeding of biomass into the reactor is not continuous, but is regulated by a rotating blade sensor which, once the wood chip level decreases, activates an auger system that transfers the wood chips from a hopper downstream of the vibrating screener to the gasifier. The inlet to the gasifier is regulated by two valves that open alternatively, introducing a finite amount of wood chips, so as to minimize unwanted air inlets at the top of the reactor, since the reactor operates at lower barometric pressure conditions in the range of  $-(3\div 8)$  mbar gauge pressure. The gasification reactor is of the fixed-bed downdraft type, with an hourglass shape. The biomass is fed into the upper part and, as it descends into the gasifier, undergoes the reactions of drying, pyrolysis, combustion, and gasification.

In the restriction zone (i.e. the throat), air is supplied through the nozzles located on the reactor circumference, driven by a fan. Locally, exothermic combustion reactions take place (although the reactor works with a lack of oxygen compared to the stoichiometric quantity), which sustain the other endothermic reactions taking place in the gasifier. All reactions take place because the system is kept under negative gauge pressure due to the suction of the internal combustion engine. By means of this pressure, the syngas, at a temperature of approximately 750 °C, is forced to pass through a grate in the lower part of the gasifier, which prevents the passage of the coarser pieces of char or wood chips, and then the syngas passes through an air-syngas countercurrent exchanger that preheats the reaction air.



**Figure. 1.** The two plants in the Synbiose area of the thermal power plant of the Campus in Parma.

The gas is then filtered through ceramic fiber filter elements (alumina silicate wool) at a temperature of approximately 600 °C. This filtration stage separates the carbon particles and char that the syngas has dragged along with it in its flow. Downstream of this filter, the gas passes through a so-called check filter, consisting of a very fine metal grid. Within this filter, a differential pressure sensor detects the fouling on the metal grid and, if a ceramic filter element has broken, it interrupts the engine operation by sending the gas to the flaring to preserve the integrity of the engine. Downstream of this element is a water-syngas heat exchanger, of the shell-and-tube type, which allows the syngas to cool down to approximately 110 °C, dropping below the dew temperature of certain classes of tar, which, as they condense, can thus be removed from the gas stream and removed from the exchanger via a double valve system.

Approximately 20 kW of heat output can be recovered from this heat exchanger. After this element, the syngas is fed into a metal filter that separates a final portion of tar (consisting of elements with a lower molecular weight than those removed previously) by coalescence and also a portion of the moisture present in the syngas. At this point, the syngas is fed into an aspirated internal combustion engine to produce electricity and heat. Under optimal conditions, up to 125 kW of electrical power and 200 kW of thermal power can be recovered from the cooling of the engine and combustion gasses. The combustion gasses then pass through a trivalent catalytic converter before being emitted into the atmosphere. A dedicated dry cooler is used to dispose of the heat output in the event of no demand from the user. Both electrical and thermal power are fed to the electricity and district heating networks that supply the University Campus, respectively.

The plant was entirely equipped with measuring instruments (Figure 2). The measured data was acquired on a quarter-hourly basis. Pressure and temperature sensors were placed upstream and downstream of each component. All temperature sensors are RTD PT100 type except for the K-type thermocouple installed for the syngas at the outlet of the gasifier (where temperatures at start-up can exceed 1100 °C). Type J thermocouples were installed up to the point downstream of the main filter, again due to the high temperatures. The pressure sensors, connected to the process via a steel capillary that protects the instrument from high syngas temperatures, are of the capacitive type with a ceramic membrane and have an operating range of (- 400 ÷ 400) mbar.

An air flow meter is placed upstream of the fan feeding air into the gasifier. Two flow meters and two temperature sensors are placed on the hot water circuits recovered on the water-syngas exchanger and on the internal combustion engine in order to measure the thermal energy exchanged.

There are also temperature sensors inside the reactor (at the top and in the central part near the nozzles) and a negative gauge pressure sensor placed at the top of the reactor. In addition, there is a differential pressure sensor located across the ceramic filter elements to assess their state of fouling and to provide periodic cleaning by means of compressed air supplied in the counterflow.

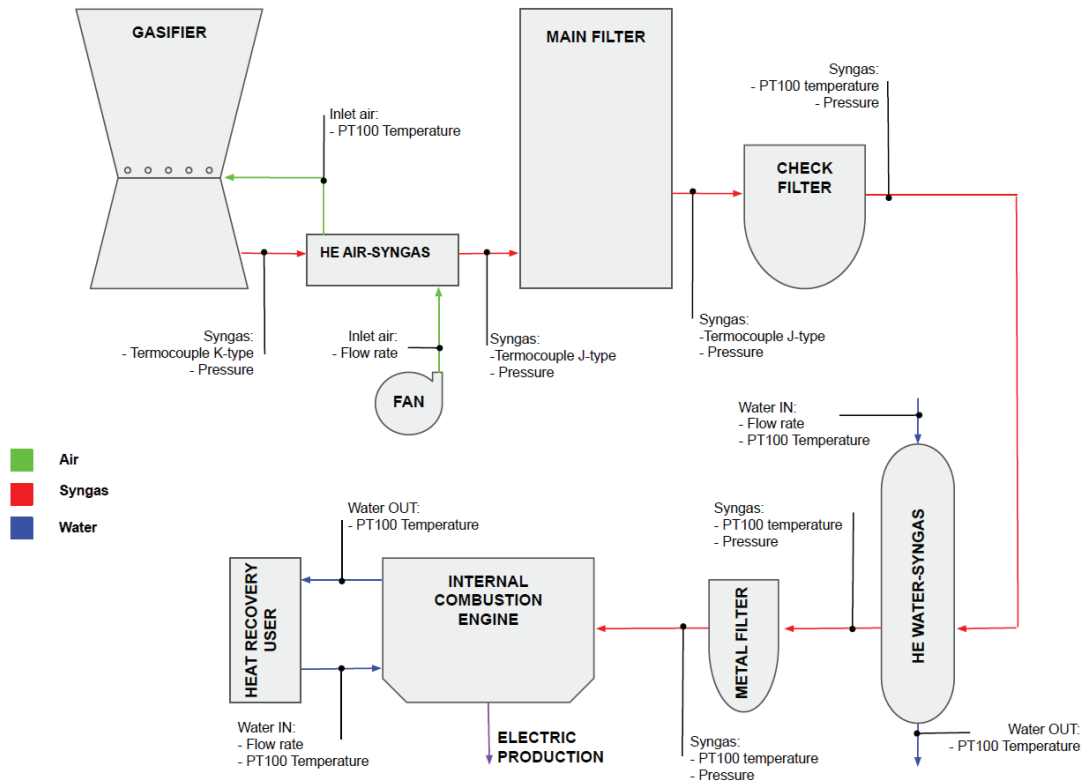


**Figure 2.** A schematic representation of the measurement points on the 125-kW plant.

Since the syngas, rich in impurities, would have compromised any measuring instrument fitted to the line, the syngas flow rate was estimated by means of an energy balance on the syngas-air exchanger. Ambient temperature and pressure sensors were installed to characterize the ambient atmosphere.

## 2.2. The 25-kW plant

Due to its smaller size and easier maintenance, a smaller plant than the previous one was used for the experimental characterization of different wood species. This plant consists of a hopper in which approximately 0,33 m<sup>3</sup> of biomass is stored, which is then fed to a downdraft reactor. At the base of this reactor is a grate shaker system that removes the thicker flakes of char and favors the advancement of the biomass. The syngas thus produced is then further purified of carbon particles first through a cyclone, then cooled through a syngas-water tube bundle exchanger and subsequently, at lower temperatures, filtered in a fabric bag filter. Before being fed into the aspirated internal combustion engine, the air-syngas mixture is filtered through a paper filter.

For the sampling of the syngas required to perform characterization analyses, a suitable sampling valve is placed downstream of the bag filter.

## 3. The experimental campaign

The two plants presented in Section 2 were used for the experimental campaign. In particular, the 125-kW plant was operated in long run sessions with the aim to monitor the performances of each component and to improve its availability that was limited by its heavy maintenance needs. The 25-kW plant instead was used to test wood chips from different tree species in order to evaluate the quality of the syngas produced.

### 3.1. Long run sessions

The 125-kW plant was monitored during its operation while feeding the electrical and district heating networks of the Campus. The electrical power output was generally kept within the range (90÷100) kW. The measurements were collected every 15 minutes and stored for elaboration. In Fig. 3a, for example, the evolution of the absolute pressure at the filters is shown for one day. The oscillations are due to the deposit of dust cake on the ceramic candles of the main filter and their jet-pulse cleaning.

Since it was not possible to directly measure the mass flow rate of the syngas, this needed to be estimated indirectly. It was decided to use the energy balance at the air-syngas heat exchanger, since the air mass flow rate, the air inlet and outlet temperature, and the syngas inlet and outlet temperature are measured.

$$\dot{m}_{syn} = \frac{\dot{m}_{air} c_{p,air} (T_{air,out} - T_{air,in})}{c_{p,syn} (T_{syn,in} - T_{syn,out})} \quad (1)$$

The resulting mass flow rate ranged between (0.06±0.10) kg/s and its evolution for one day is reported in Fig. 3b, confirming that the oscillations in pressure at the check filter were not due to a variation in mass flow rate.

The data gathered from the experiment have been used to train and validate the models presented in Paragraphs 4.2 and 4.3 and to evaluate health indices regarding the different components (e.g. pressure loss coefficient on filters and pipes, as shown in Fig. 4 for the ceramic candles).

### 3.2. Syngas characterization

The 25-kW plant was used to test 8 different tree species dried both naturally and artificially. The wood chips were sampled before the test. Then the elemental analysis and the evaluation of the ash content, of the moisture, and of the lower heating value on a dry basis were performed. The result of this characterization is reported in Table 1.

The test was then performed by feeding the 25-kW plant and keeping it at a constant electrical power output (i.e. 7.5 kW) until a steady state was reached. The syngas was then sampled with a Tedlar bag and analyzed through gas chromatography–mass spectrometry. Table 2 presents the results in terms of mass fraction of carbon monoxide, hydrogen, methane, carbon dioxide, hydrogen sulfide, oxygen, and nitrogen in the anhydrous syngas. Moreover, the water and tar content and the lower heating value is reported.

It can be noted that the data do not show any significant correlation between the characteristics of the biomass and those of the produced syngas.

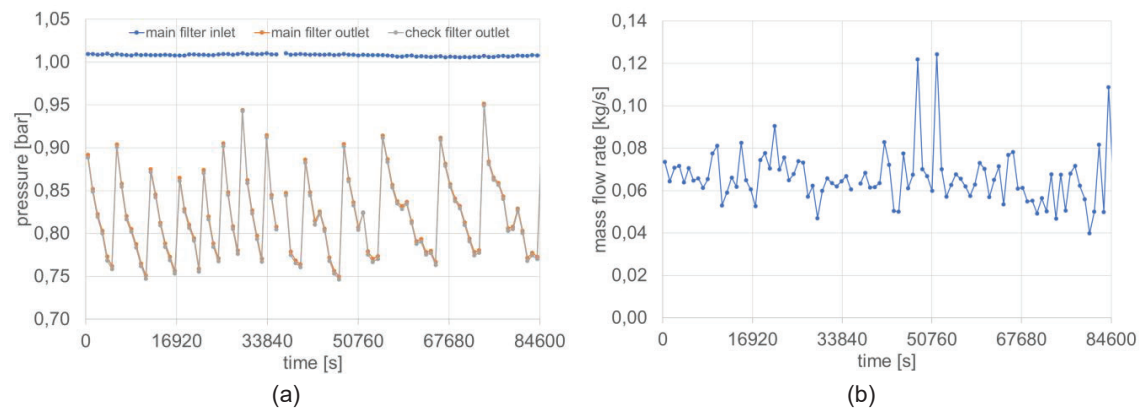


Figure 3. Evolution of pressures (a) and syngas mass flow rate (b) in a sampled day.

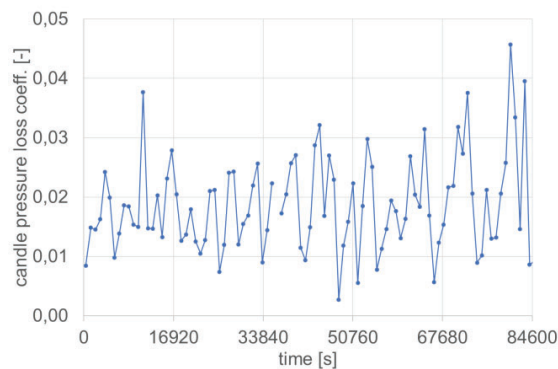


Figure 4. Evaluation of the pressure loss coefficient on the ceramic candle in the main filter.

**Table 1.** Results of the wood chip characterization.

Tree species	Drying	C	H	O	N	S	Ash	Moisture	LHV
		%	%	%	%	%	%	%	kJ/kg
Chestnut	Natural	46,5	2,6	49,7	0,4	0,4	0,5	22,0	17350
Cherry	Natural	N/A	N/A	N/A	N/A	N/A	N/A	N/A	N/A
Beech	Natural	45,8	5,7	46,9	0,7	0,1	0,8	8,7	17740
Walnut	Natural	45,0	0,6	53,0	0,3	0,1	1,1	31,0	18100
Pine	Natural	N/A	N/A	N/A	N/A	N/A	N/A	N/A	N/A
Poplar	Natural	44,7	5,7	48,3	0,1	0,1	1,0	16,0	17730
Black locust	Natural	48,0	3,6	46,9	0,2	0,1	1,2	18,0	11080
Durmast	Natural	43,9	5,0	48,0	0,4	0,1	2,7	18,0	N/A
Chestnut	Artificial	47,8	5,9	45,2	0,4	0,1	0,7	2,5	16370
Cherry	Artificial	47,1	6,1	46,0	0,1	0,1	0,6	1,1	15473
Beech	Artificial	39,2	5,0	54,7	0,2	0,1	0,8	5,1	16710
Walnut	Artificial	42,6	5,4	50,7	0,1	0,2	1,1	7,5	16128
Pine	Artificial	44,3	5,3	50,3	0,0	0,1	< 0,5	6,5	18290
Poplar	Artificial	47,5	5,6	45,0	0,2	0,2	1,5	0,9	N/A
Black locust	Artificial	46,4	5,8	46,2	0,7	0,1	0,7	< 1,0	N/A
Durmast	Artificial	44,6	5,8	46,7	0,6	0,1	2,2	< 1,0	16570

**Table 2.** Results of the syngas characterization.

Tree species	Drying	CO	H <sub>2</sub>	CH <sub>4</sub>	CO <sub>2</sub>	H <sub>2</sub> S	O <sub>2</sub>	N <sub>2</sub>	H <sub>2</sub> O	Tar	LHV
		%	%	%	%	%	%	%	g/Nm <sup>3</sup>	mg/Nm <sup>3</sup>	MJ/Sm <sup>3</sup>
Chestnut	Natural	18,6	27,5	2,8	12,8	0,6	1,1	36,4	19,6	4457	6,41
Cherry	Natural	N/A	N/A	N/A	N/A	N/A	N/A	N/A	N/A	N/A	N/A
Beech	Natural	14,6	24,1	3,3	10,7	0,7	2,7	42,8	42,9	37717	7,13
Walnut	Natural	15,3	29,6	2,9	15,0	0,3	0,5	36,4	53,5	1793,1	6,23
Pine	Natural	N/A	N/A	N/A	N/A	N/A	N/A	N/A	N/A	N/A	N/A
Poplar	Natural	15,0	25,4	2,6	11,7	0,1	3,1	41,8	31,5	17310	5,83
Black locust	Natural	20,6	21,4	3,0	14,2	0,1	0,8	39,8	35,3	5678	6,55
Durmast	Natural	17,5	23,8	3,1	11,8	0,3	2,3	41,2	28,2	2271	5,58
Chestnut	Artificial	17,8	29,3	3,5	14,2	0,4	1,8	33,0	63,8	841	6,31
Cherry	Artificial	18,6	24,1	2,7	17,3	0,6	1,0	35,7	29,9	2713	5,61
Beech	Artificial	19,7	27,4	3,6	16,1	0,8	1,4	31,0	62,9	9922	6,52
Walnut	Artificial	19,7	22,2	2,8	11,4	0,3	2,6	41,1	36,8	2241	5,57
Pine	Artificial	20,1	24,0	4,0	16,9	0,7	1,5	32,8	66,0	11524	6,21
Poplar	Artificial	24,3	24,0	3,1	8,0	0,1	1,8	38,7	37,4	5447	6,41
Black locust	Artificial	18,0	26,4	3,5	17,6	0,9	1,1	32,3	61,6	7151	6,45
Durmast	Artificial	18,6	28,2	3,4	14,4	0,4	1,6	32,5	64,5	37298	7,67

## 4. The simulation campaign

### 4.1. Gasification process

A model for the simulation of the gasification process that takes place in a fixed-bed downdraft gasifier was developed and implemented in Scilab. The model combines a lumped parameter stoichiometric equilibrium model for the pyrolysis and oxidation zones with a one-dimensional kinetic model for the reduction zone.

In particular, the former takes into consideration two reactions, i.e. water gas shift (R1) and char methanation (R2), which are assumed to be at the equilibrium. The molar fraction of each species at the outlet of the pyrolysis and oxidation zones are constrained by the mass balances of each element (i.e. C, H, O) and by the ratio given by the equilibrium constants (Eq. 2):



$$K = \frac{\prod_{products} x_p^{s_p}}{\prod_{reactants} x_r^{s_r}} \quad (2)$$

The value of the equilibrium constant for each reaction is calculated through Eq. 3, where the temperature is determined by means of the energy balance in the pyrolysis and oxidation zones.

$$K = e^{-\frac{\Delta G^0}{RT}} \quad (3)$$

The kinetic model for the reduction zone, takes into consideration four reactions.





The rate of each reaction is evaluated through Eq. 4, where the equilibrium constant is calculated as seen before with Eq. 3 and the energy balance, for each control volume into which the reduction cone is divided. The net formation/destruction rate of each species is calculated considering all the reactions in which the species participates.

$$r = C_{RF} A e^{-\frac{E}{RT}} \left( \prod_{reactants} x_r^{S_r} - \frac{\prod_{products} x_p^{S_p}}{K} \right) \quad (4)$$

The model is validated by applying it to a literature test case [7]. The main input data are reported in Table 3, and the output data in Table 4. It can be noticed that the results are satisfactory for the species (H<sub>2</sub> and CO) responsible for the lower heating value of the syngas.

#### 4.2. System simulations

A comprehensive 0D lumped parameter dynamic model was developed for the simulation of the whole system (i.e. gasifier, syngas cleaning line and engine) and it was implemented in Matlab®/Simulink® by assembling component models. The model is based on the energy and mass balances for each component. Some of the components are considered as capacities (in green in Fig. 5a) and the balances are implemented with integral equations allowing for mass and energy storage. On the other hand, there are the resistances (in orange) with the balances implemented with algebraic equations. Particular care has been devoted to syngas conductivity, density, specific heat capacities and viscosity calculation. The model is able to simulate the behavior of the system both under stationary and transient conditions (e.g. the pressures before and after cleaning are shown in Fig. 5b). The most significant results are presented in [8, 9], showing that the model is a valuable tool for the diagnosis of the syngas cleaning line.

**Table 3.** Input of the gasification model for the validation [7].

Power	Fixed Carbon	Volatile Matter	Ash	C	H	O	S	N	Moisture	Biomass mass flow rate	Air to fuel ratio
[kW]				[g/100 g dry basis]						[g/s]	[g air/g biomass]
4										8,1	1,37
6										10,2	1,48
8	16,51	79,84	3,65	45,19	5,74	44,92	0,44	0,06	7,02	12,1	1,63
10										12,4	1,69
12										12,9	1,79

**Table 4.** Output of the gasification model and comparison with experimental data from the literature [7].

Power	Simulation					Experimental					Error (Sim. - Exp.)				
	H <sub>2</sub>	CO	CO <sub>2</sub>	CH <sub>4</sub>	N <sub>2</sub>	H <sub>2</sub>	CO	CO <sub>2</sub>	CH <sub>4</sub>	N <sub>2</sub>	H <sub>2</sub>	CO	CO <sub>2</sub>	CH <sub>4</sub>	N <sub>2</sub>
[kW]	[%mol/mol]					[%mol/mol]					[%mol/mol]				
4	18,9	17,4	13,8	0,1	49,8	15,4	17,3	6,9	3,4	56,9	3,5	0,1	6,9	-3,3	-7,1
6	17,1	17,4	13,5	0,0	52,0	15,3	17,2	7,0	3,4	57,2	1,8	0,2	6,5	-3,2	-5,2
8	15,2	17,3	13,2	0,0	54,3	15,1	17,0	7,2	3,0	57,8	0,1	0,2	6,1	-3,0	-3,5
10	14,7	17,2	13,1	0,0	55,0	14,9	17,0	7,2	2,8	58,1	-0,2	0,3	5,9	-2,8	-3,1
12	13,9	17,2	13,0	0,0	55,9	14,8	16,9	7,3	2,8	58,3	-0,9	0,3	5,7	-2,8	-2,4

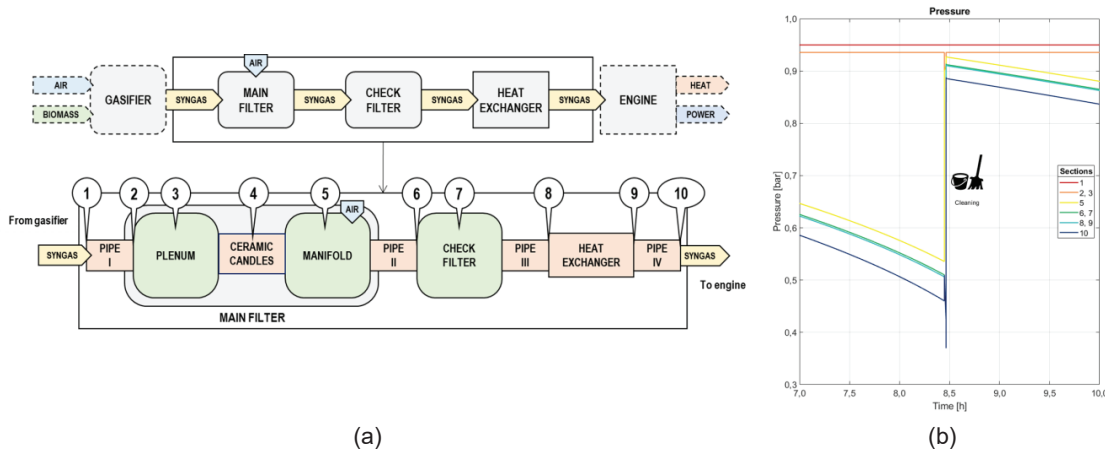


**Figure 5.** A schematic representation of the model (a) and the evolution of the simulated pressure when cleaning occurs (b) [9].

### 4.3. Component CFD simulations

An integrated 0D-3D approach is a methodology which combines a simplified thermodynamic 0D lumped parameters model (such as the one presented in Paragraph 4.2) with 3D CFD simulations. The 0D model is then able to describe the entire process by integrating information obtained by a detailed 3D CFD simulation of the individual components (such as performance maps, pressure drops, etc.). This information may be unknown or can be known with high uncertainty (for instance, from empirical correlation) and, thus, this procedure consents to obtain the set-up coefficients of the 0D models. Moreover, by means of the CFD simulation, it is possible to study the behavior of the specific components in detail in order to debug design weakness and optimize their operation. In a more sophisticated approach, then, the 0D and 3D models can actively interact as follows: the 0D model calculates the thermodynamic quantities and flow rates in the characterizing sections; it supplies them to the 3D models as the boundary conditions on which to carry out the simulation and to return the performance of the components to the 0D model; then the 0D model recalculates the thermodynamic quantities and flow rates through the balance sheets. This methodology offers a series of advantages, combining the speed and robustness of the 0D simulation model of the system with the complexity and accuracy of the 3D numerical fluid dynamics simulation. The most relevant results related to three of the most relevant components of the 125-kW plant (see Fig. 2) were the following:

- the gasifier, where the focus was on the inside (consequent to gasification reactions) and outside (consequent to the coupling with the environment) fluid dynamics and heat exchange processes;
- the syngas feeding duct, where the focus was on the fouling phenomena and on the consequences of the residual tar carried by the syngas;
- the water-syngas heat exchanger, where the focus was on both of the above topics, i.e. the internal and external fluid dynamics and heat exchange processes, and the fouling issues due to the cooling of the syngas through the heat exchanger.

#### 4.3.1. Gasifier

The downdraft gasifier was simulated by means of the two commercial finite volume CFD codes of the ANSYS platform. The preliminary results obtained with FLUENT are reported in [10]. Subsequently, by acquiring the real geometry with a reverse engineering CAD-based methodology which make use of a 7-axis laser scanner, it was possible to verify that the gasifier worked as a “quasi-throatless” downdraft principle, and it was also possible to simulate the actual geometry by means of CFX. An interesting result is reported in Fig. 6, in which it is possible to appraise the influence of the grate on the internal temperature from a distribution point of view. Even though there is a restriction, the grate shifts the operation of the gasifier from throated to throatless. This can be seen from the variation of the temperature profile near the restriction which shifts from a typical throated profile (blue line) to a typical throatless profile (red line), as seen in [11]. Moreover, the influence of the grate can also be seen from a quantitative point of view, i.e. the calculated average temperature of the exhaust gases passes from 1148 °C (without grate) to 839 °C (with grate). It is also interesting to notice that the CFD calculation is in agreement with the experimental results  $T_{syn} = 750$  °C (about 10 %).

#### 4.3.2. Syngas feeding duct

The syngas feeding duct was simulated by means of the open-source finite volume CFD code OpenFOAM. In [12], the numerical methodology developed based on a mesh-morphing algorithm is presented. The analysis made it possible to estimate the amount, rate, and area of tar deposition on the duct, which was simulated as a mixture of 5 tar classes characterized by different concentration and dew points. In Fig. 7a, by comparing a take-over on a section of the actual duct and the numerical result in terms of deposition (grey area) in the same section, it can be noticed how the numerical simulation was able to capture the shape and amount of deposition. Subsequently, the same methodology was used to estimate the increase in duct pressure drop caused by the growth of the deposit over time (Fig. 7b). In this manner, the pressure drop in the duct module of the 0D model can be updated during the life of the plant.

#### 4.3.3. Water-Syngas heat exchanger

The Water-Syngas heat exchanger geometry was also acquired on the real plant by means of reverse engineering methodology. The geometry (which is a vertical shell-and-tube heat exchanger) was then simulated by means of ANSYS CFX in clean and degraded conditions, the latter obtained by generating a modified domain according to on-field inspection of the device after several operating hours. The implanted faults were fouling (50 % area reduction of 21 tubes) and clogging (38 % of tubes fully blocked by tar solidification) [13]. The analysis showed how fouled and clogged conditions caused a decrease in heat exchanger effectiveness, an increase in pressure drop and a decrease in the capability of the heat exchanger to condense tar and separate it from the gas stream (which is the second most important function of the heat exchanger). The outcome of the simulation was also to characterize the performance of the heat exchanger which was not provided by the manufacturer since the heat exchanger was designed ad hoc and built on site. This characterization was used to feed the 0D model, as described below.

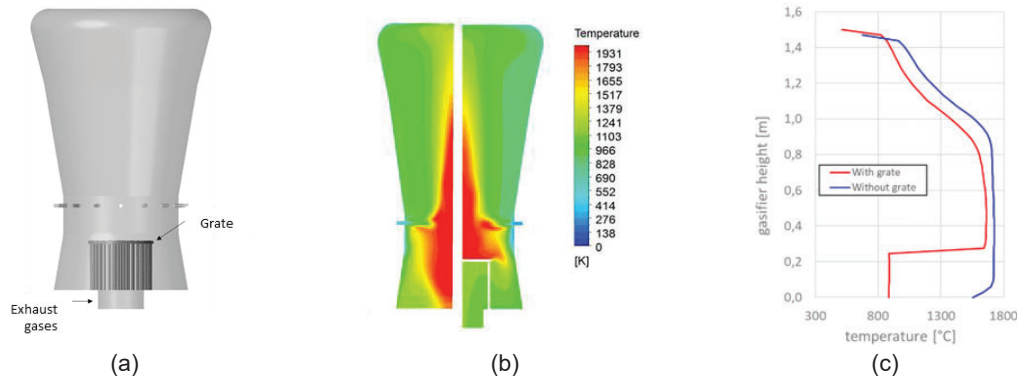


**Figure 6.** Gasifier geometry (a), temperature distribution without grate on the left and with grate on the right (b) and temperature profile (c).

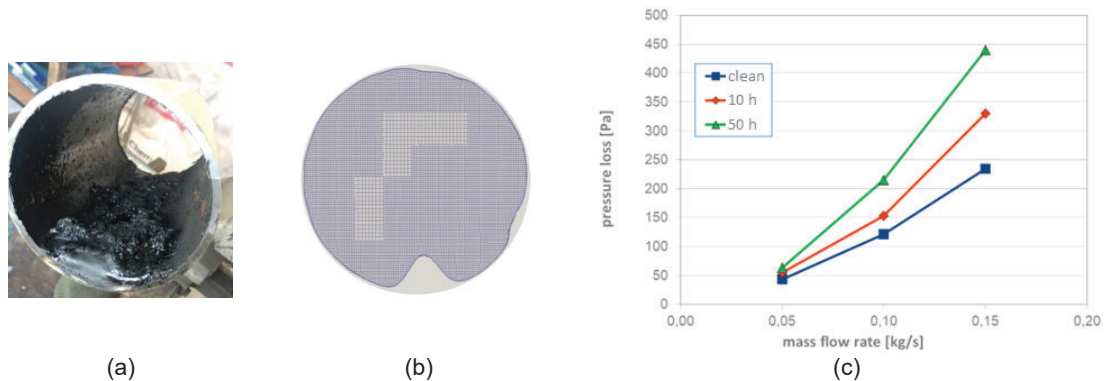


**Figure 7.** Actual tar deposit (a), numerical tar deposit (b) and pressure drop curves as a function of elapsed time (c).

#### 4.4. 0D-3D model integration

As depicted in Fig 8., by taking advantage of the CFD characterization described above, the 0D model can be fed by the obtained numerical 3D results to make the plant simulation more realistic. In the Figure, the interaction between the syngas feeding duct numerical 3D simulation and the 0D model are outlined.

### 5. Discussion

The project promoted the penetration of a renewable source technology, which is efficient as it is cogenerative, into a portion of the market (the tertiary sector) which is currently almost exclusively the domain of photovoltaic technology. Another impact on the national power system is the reductions in both climate-altering emissions (reduction in carbon dioxide emissions as renewable and cogeneration source technology) and pollutant emissions (by using biomass-derived fuels in internal combustion engines there is a reduction in pollutant emissions compared to direct biomass combustion). By experimenting with the potential expansion of the use of virgin and residual biomass blend technology, the research program has enabled the expansion of the technology to the use of residual biomass resulting in the increased sustainability of the supply chain. Finally, it should be emphasized that the diffusion of a technology such as the one being tested allows for an increase in the share of electricity produced from renewable sources without affecting the stability of the electricity grid as the technology is programmable. These benefits for the grid are amplified by the fact that it is a distributed generation technology with simultaneous self-consumption. Therefore there is no significant power transmission and it consequently decongests the grid.

After more than five thousand hours' monitoring the 125-kW plant, it can be stated that this kind of plant, although functioning from a technical point of view, has not yet reached a technological maturity allowing it to be operated continuously without continuous close monitoring. It requires costly and constant maintenance, with many variables that can affect the performance of the system, beginning with the quality of the wood chips.

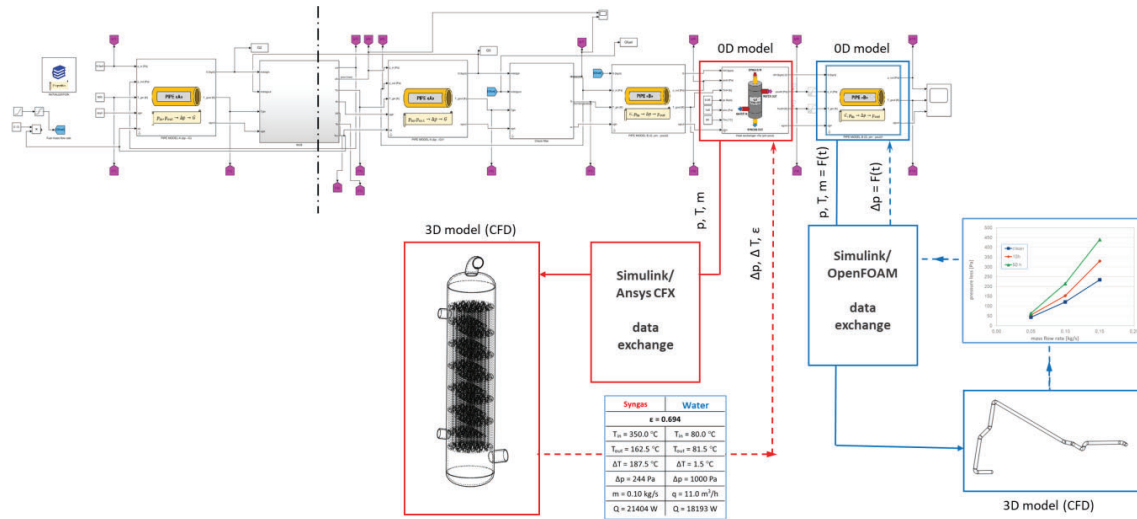


**Figure 8.** 0D-3D methodology concept: interaction between the heat exchanger and syngas feeding duct 3D model results and the 0D lumped parameter model.

Since the raw material is inhomogeneous by nature, it is impossible to find standard operating conditions, as would be the case for a natural gas-fired plant. In addition, tar deposition creates major problems that require constant maintenance and cleaning. The cleanliness of the syngas, in terms of tar content, therefore, remains the point on which to focus research in order to make the plants more manageable.

It would be interesting to be able to feed the plants with residual biomass instead of virgin wood chips, e.g. those recovered from agricultural or forestry activities, to lower the cost of the feedstock. From an economic point of view, in fact, such plants can only be sustained in a context where there are incentives for the sale of energy.

### 5.1. Implemented plant improvements

Following an initial phase in which the plants were operated as delivered by the manufacturers, the following improvements were implemented:

- Substitution of the flaring torch with one more suitable for syngas, which has large passage sections, especially on the flame arrestor, to limit pressure drops because of tar condensation on this component. Moreover, to process syngas, a centrifugal fan with backward-curved blades and wide clearance between the case and rotor was adopted, so that any tar deposits would not compromise the functionality of the machine. Finally, the torch, compared to what was originally planned, was supplemented with support gas, to facilitate the ignition of the gas when it was still poor in the initial ignition phases, which also helped to limit the fouling of the torch itself;
- Insertion of a calm chamber upstream of the flare fan to limit the dust processed by the fan;
- Insertion of a metal filter upstream of the engine, to limit the presence of tar in the combustion chamber. Tar, if not burnt inside the engine cylinders, can condense as a result of low temperatures after mixing with air, creating a sticky layer that compromises engine functionality. A high molecular weight tar class condenses in the syngas-water exchanger; due to temperatures above around  $105\text{ }^{\circ}\text{C}$ , light-weight tar and water content do not condense in the heat exchanger. This metal filter, which operates at lower temperatures, allows the condensation of the moisture component and, by coalescence, the removal of a further proportion of the tar. This filter consists of a packed metal fiber. It preserves the life of the engine which, in the overall balance of the system, is a delicate and expensive component.

### 5.2. Designed improvements

Other solutions have been designed to further improve the plant, but they have not yet been implemented:

- Insertion of a cyclone between the gasifier and the main filter. By adopting this solution, it would be possible to eliminate an initial portion of carbon residues and thus relieve the ceramic filters of some of the fine dust. In this way, the frequency of pulsejet cleaning with compressed air would decrease, thus guaranteeing fewer interruptions to production and increasing the life of the filters. These filters tend to become fragile and break as a result of pulsejet cleaning; the cost of these components is not negligible and the intervention of stopping to replace them is rather onerous, so limiting the frequency of these occurrences would bring a significant benefit.

- Increasing the size of the filter case, by adding additional filter elements, would bring a benefit in terms of the quality of the syngas fed to the engine.
- It could be useful to include an ash/char removal system from the bottom of the gasifier, as is already present in the filter case, so that the frequency with which reactor cleaning is carried out can be reduced. In fact, this operation, carried out every 250 hours at the same time as the maintenance of the internal combustion engine, takes a long time (usually a couple of days) so that the system can cool down and be accessible by the operators. Doing so would also improve the general cleanliness, positively affecting the operational stability of the entire system.
- Following the CFD study, it was shown that the heat exchanger is not optimized and only condenses the tar in the last section of the tube bundle. Optimizing its fluid dynamics or simply adopting a longer heat exchanger could allow even more tar to be removed and feed a cleaner syngas to the engine.
- Increasing the cross-section of the piping, in addition to reducing pressure drops in general, could make it possible to reduce the frequency of any maintenance work, which entails disassembling the piping to remove any solidified tar that is obstructing the syngas passage.
- The flame arrestor serving the safety flare has very small gas passage sections and is extremely sensitive to the presence of tar. The deposition of tar on it leads to its complete obstruction with consequent problems for the functionality of the flare and safety problems in general, since the gas cannot find an outlet to the outside. The adoption of a hydraulic guard system, while bringing with it the burden of disposing of contaminated process water, would solve the problem of the fouling of the arrestor, which could be removed, itself representing an anti-backfire system. This would feed filtered syngas to the flare from the hydraulic stop, improving its performance.

## Acknowledgments

The work was carried out within the framework of the research project "SYNBIOSE - Gassificazione di biomasse lignocellulosiche in sistemi di cogenerazione di piccola taglia (<200 kW) per applicazioni nel settore terziario" (CUP G96G16000800003) funded by "Cassa per i servizi energetici e ambientali" within the call "Bando di gara per progetti di ricerca di cui all'art. 10, comma 2, lettera b) del decreto 26/1/2000, previsti dal Piano triennale 2012–2014 della ricerca di sistema elettrico nazionale e dal Piano operativo annuale 2013."

## Nomenclature

$A$	pre-exponential factor, $s^{-1}$
$c$	specific heat, $J/(kg\ K)$
$C_{RF}$	char reactivity factor [14]
$G$	Gibbs free energy, $J/mol$
$K$	equilibrium constant
LHV	lower heating value, $kJ/kg$ or $MJ/Sm^3$
$\dot{m}$	mass flow rate, $kg/s$
$R$	gas constant, $J/(mol\ K)$
$r$	reaction rate, $s^{-1}$
$s$	stoichiometric coefficient
$T$	temperature, $^{\circ}C$ or $K$
$x$	molar fraction

### Subscripts and superscripts

$air$	air
$in$	inlet
$out$	outlet
$p$	product
$r$	reactant
$syn$	syngas

## References

- [1] Ahmad, A. A., Zawawi, N. A., Kasim, F. H., Inayat, A., & Khasri, A., Assessing the gasification performance of biomass: A review on biomass gasification process conditions, optimization and economic evaluation. *Renewable and Sustainable Energy Reviews* 2016;53:1333-1347.
- [2] Azzone, E., Morini, M., Pinelli, M., Development of an equilibrium model for the simulation of thermochemical gasification and application to agricultural residues. *Renewable energy* 2012;46:248-254.

- [3] Gambarotta, A., Morini, M., Zubani, A., A non-stoichiometric equilibrium model for the simulation of the biomass gasification process. *Applied Energy* 2018;227:119-127.
- [4] Havilah, P. R., Sharma, A. K., Govindasamy, G., Matsakas, L., & Patel, A., Biomass Gasification in Downdraft Gasifiers: A Technical Review on Production, Up-Gradation and Application of Synthesis Gas. *Energies* 2022;15(11):3938.
- [5] Patuzzi, F., Prando, D., Vakalis, S., Rizzo, A. M., Chiaramonti, D., Tirlir, W., Mimmo, T., Gasparella, A., Baratieri, M., Small-scale biomass gasification CHP systems: Comparative performance assessment and monitoring experiences in South Tyrol (Italy), *Energy* 2016;112:285-293.
- [6] Stamponi, E., Giorgini, F., Cotana, F., Moretti, E., Preliminary assessment of a microgrid integrated with a biomass gasification CHP system for a production facility in Central Italy, *E3S Web of Conferences* 2021;238:01012.
- [7] Mazhkoo, S., Dadfar, H., HajiHashemi, M., Pourali, O., A comprehensive experimental and modeling investigation of walnut shell gasification process in a pilot-scale downdraft gasifier integrated with an internal combustion engine, *Energy Conversion and Management* 2021;231:113836.
- [8] Gambarotta, A., Manganeli, M., Morini, M., A model for filter diagnostics in a syngas-fed CHP plant. *Energy Procedia* 2018;148:400-407.
- [9] Gambarotta, A., Manganeli, M., Morini, M., A model for the simulation of the gas cleaning system in a syngas-fed CHP plant. *AIP Conference Proceedings* 2019;2191(1):020084.
- [10] Vulpio, A., Casari, N., Morini, M., Pinelli, M., Suman, A., Numerical investigation of a wood-chip downdraft gasifier. *E3S Web of Conferences* 2019;113:01002.
- [11] Basu, P., Biomass Gasification, Pyrolysis and Torrefaction (Third Edition), Academic Press; 2018.
- [12] Casari, N., Pinelli, M., Suman, A., Candido, A., Morini, M., Deposition of syngas tar in fuel supplying duct of a biomass gasifier: a numerical study. *Fuel* 2020;273:117579.
- [13] Aldi, N., Casari, N., Pinelli, M., Suman, A., Vulpio, A., Performance Degradation of a Shell-and-Tube Heat Exchanger due to Tar Deposition. *Energies* 2022;15(4):1490.
- [14] Sharma, A. K., Equilibrium and kinetic modeling of char reduction reactions in a downdraft biomass gasifier: A comparison. *Solar energy* 2008;82(10):918-928.